

ON THE INFLUENCE OF LOW-ENERGY IONIZING RADIATION ON THE AMINO ACID MOLECULE: VALINE CASE

J. Tamulienė^a, L. Romanova^b, V. Vukstich^b, A. Papp^b, L. Baliulytė^a, and A. Snegursky^b

^a*Institute of Theoretical Physics and Astronomy, Vilnius University, Saulėtekio 3, 10222 Vilnius, Lithuania*

^b*Institute of Electron Physics, National Academy of Sciences of Ukraine, 21 Universitetska Street, 88017 Uzhgorod, Ukraine*

Email: jelena.tamuliene@tfai.vu.lt

Received 2 November 2017; revised 19 December 2017; accepted 21 June 2018

New data on the valine molecule ($C_5H_{11}NO_2$) fragmentation under the low-energy electron-impact are presented. These data are related to the formation of ionized products due to the ionizing radiation influence on the above amino acid molecule. A series of the fragments produced are identified by applying an extensive DFT-theory approach. The results obtained allowed the principal pathways of the valine molecule fragmentation to be found. The absolute appearance energies of some fragments are both measured experimentally and calculated theoretically. The experimental and theoretical data are compared and analysed.

Keywords: valine, ionizing radiation, mass spectrum, fragmentation

PACS: 31.15. A, 33.15.Ta, 34.80.Ht

1. Introduction

Currently, the radiation-implication-study of amino acids is a focus for researchers due to the fundamental importance of these molecules – building blocks of proteins. It is known that low-energy electrons, representing the most predominant species formed during a very short time after the deposition of high energy ionizing quanta into a biological medium, produced by primary ionizing radiation penetrating a biological tissue, can effectively damage the biologically relevant molecules of the human body [1]. The interaction of these electrons with the above molecules can induce mutagenic and genotoxic lesions [2–4].

The obtained results on the electron–biomolecule collisions under isolated conditions have one decisive drawback for the interpretation of possible processes in complex macromolecules [5]. In this case, the environmental influence by neighbouring molecules or water that can modify the electron scattering processes is

neglected, although it could alter structures, stabilities and function of biological macromolecules [6]. Our approach is to extend the earlier studies on the isolated molecules in the gas phase and to study the fragmentation of the most stable and, consequently, more abundant conformational isomers of the molecules under investigation. Our recent study indicates that conformational isomerism may influence the near-threshold areas of the dissociative ionization cross-sections [7]. Moreover, the presence of intramolecular hydrogen bonds and the differences in the locations of certain atoms in the conformational isomers may lead to the changes in the fragment appearance energies up to 2 eV.

Here we report on the interaction of low-energy (<70 eV) electrons with valine conformational isomers in order to probe the intrinsic properties of this molecule and to trace its change(s) under the electron impact. This work is a continuation of a series of our studies on the ionizing radiation interaction with the molecules of biological

relevance. The goal of our studies was to elucidate the major channels of formation of the most stable valine molecule conformers as a result of the low-energy electron impact.

Valine is an α -amino acid used in the protein biosynthesis. Besides the α -amino and α -carboxylic acid groups, it also contains the side chain isopropyl variable group, classifying it as a non-polar amino acid. It is essential for humans, i.e. the body cannot synthesize it and, thus, it must be obtained from the diet. Human dietary sources are any proteinaceous foods such as meats, dairy products, soy products, beans, and legumes.

Along with leucine and isoleucine, valine is a branched-chain amino acid. In sickle-cell disease, valine substitutes for the hydrophilic amino acid glutamic acid in β -globin. Because valine is hydrophobic, the hemoglobin is prone to abnormal aggregation.

2. Experiment

The experimental apparatus on the basis of a serial MI1201 magnetic mass spectrometer has been described in detail in our previous papers (see, e.g. [7, 8]). Here we shall only briefly state that it operated within the $m/z = 1\text{--}600$ a.m.u. range (here m/z is the mass to charge ratio of the ions under study) at high sensitivity ($\sim 10^{-16}$ A) and resolution (± 0.25 a.m.u.), enabling reliable separation and detection of the fragments of the target molecule [8–10]. The beam of the valine molecules was formed by means of a resistively heated effusion source with the molecule concentrations of about 10^{10} molecule/cm³. The operating temperature of the molecular beam source was varied up to 150°C providing conditions excluding the initial molecule thermal degradation and molecular cluster formation. A specially designed three-electrode electron gun provided an electron current of 30–50 μ A over a wide (0–150 eV) energy range. This source enabled the energy dependences of the ionization and dissociative ionization cross-sections to be measured in the incident electron energy range from the threshold up to 150 eV without the need of using a magnetic field (contrary to the conventional source). The ions produced in the ion source and extracted by the electric field entered the magnetic ion separator and were detected by means of an electrom-

eter. The data acquisition and processing system was controlled by a PC. Special measures have been applied to stabilize the mass analyzer transmission, and to make the mass of the fragment under study to be reliably fixed. An electron energy scale was calibrated with respect to the known ionization thresholds for the argon atom and nitrogen molecule with the accuracy of ± 0.1 eV [7]. The valine molecule mass spectrum was measured at the 70 eV electron energy, the appearance energies for the positive fragment ions were determined within the 5–30 eV energy range with the ± 0.1 eV accuracy.

3. Theory

The study was performed by the Becke's three-parameter hybrid functional applying the non-local correlation provided by Lee, Yang and Parr (B3LYP) [11], i.e. a representative standard DFT method with the cc-pVTZ basis implemented in the Gaussian and GAMESS packages [12–14]. The given set was suitable to describe the system under study with computations being performable. We used a contracted basis set taking into account the correlation effects with a (12s6p) primitive basis set contracted under the Raffanetti pathway and optimized at the Hartree-Fock (HF) level because this basis set demonstrated an excellent behaviour for calculating both atoms and molecules. Moreover, this relatively large basis set and electron correlation correction are good enough to study the interactions with hydrogen-bound complexes.

The structures of the five conformers of the neutral valine molecule were optimized without any symmetry constraint. Referring to the results on the total energy and molar distribution at 433 K, the two most stable conformers were chosen for the further investigation. In order to model the fragmentation processes, the fragment anions, cations and fragments with a zero charge were evaluated, i.e. the neutral dissociation, dissociative ionization and bipolar dissociation (ion pair formation) were studied. The spin multiplicity of the closed-shell products of the reactions under investigation was 1, while that of the open shell was 2. The comparison of the experimental measurements and theoretical calculation of the energy of the fragment appearance proved that the chosen spin states were enough to describe

the most probable reactions of fragmentation. The ionization potential was calculated as the difference of the energies of the neutral and positively charged conformer.

The appearance energies were calculated as the difference between the total energy of the investigated conformer of the molecule and the sum of the energies of the fragments predicted. The calculated values of the dissociation energy were compared with those of the experimental measurements to select and present more probable reactions of the fragment appearance. The vibration analysis of the compounds under study was performed to estimate the zero point corrections. These corrections were not included due to their insignificance.

4. Results and discussion

Valine, like most amino acids, exists in two possible optical isomers called the D- and the L- isomers. The L-amino acids represent the vast majority of them found in proteins. It is the main reason why only the L-optical conformers are under our study. Geometric structures of these conformers are different due to one of the following reasons:

- the carboxylic acid group rotates, and the acid hydrogen may be oriented towards amino nitrogen or away from it;
- the methyl groups rotate, and the methyl hydrogen may be oriented towards the carboxylic acid.

In Ref. [15], the calculations of the global energy minimum for the gas phase valine were

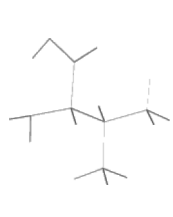
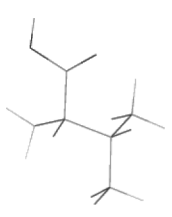
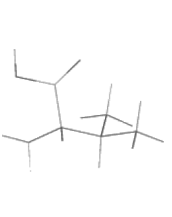
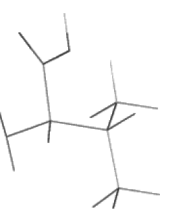
analysed briefly. It was shown that different calculation methods do not provide an unambiguous determination of the lowest-energy valine conformer. However, the two distinct structures corresponding to the global energy minima with the hydrogen bonding accounted correspond to the bifurcated $\text{NH}_2 \cdots \text{O}=\text{C}$ and the $\text{N} \cdots \text{H}-\text{O}$ hydrogen-bonded valine molecules. In addition, the authors of the above paper underlined that the rotation of the isopropyl side chain around the α -C axes led to a number of rotamers for each of these conformers, all of which were close to the global energy minimum.

Our calculations show that the structural difference insignificantly affects the stability of the conformers (further referred to as Valine 1, Valine 2, Valine 3 and Valine 4), i.e. their total energies are not very different. Only the total energy of Valine 3 is 0.080 eV higher than that of other conformers, while in other cases the total energy differences are lower than the energy of the thermal movement.

However, the molar abundance at $T = 433$ K that corresponds to the experimental temperature is notably different (see Table 1). Valine 1 and Valine 4 represent the vast majority of the conformers under investigation. Hence, here we present the results of the studies on the fragmentation of these two most abundant conformers, although additional data on the fragmentation of the rest of conformers could be provided as well.

The images of the two main valine conformers and the atom numbers, used in this paper, are presented in Fig. 1. We call the conformers Valine 1 (on the left) and Valine 4 (on the right). Note that

Table 1. Total energies of the neutral and ionized valine conformers, their ionization energies and the molar distribution at $T = 433$ K.

	Valine 1	Valine 2	Valine 3	Valine 4
				
Total energy, neutral molecule, a.u.	-402.367	-402.366	-402.364	-402.367
Total energy, ionized molecule, a.u.	-402.045	-402.057	-402.054	-402.059
Molar distribution at 433 K, %	45.21%	17.18%	5.44%	32.17%
Ionization energy, eV	8.814	8.399	8.482	8.448

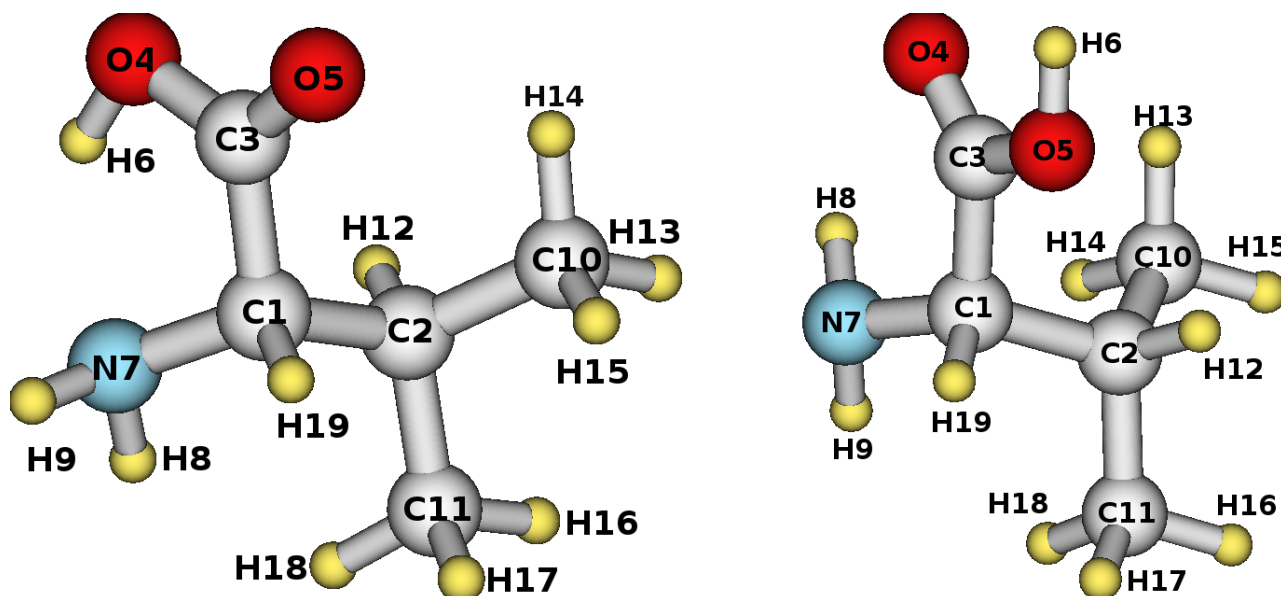


Fig. 1. Views of conformers of Valine 1 (on the left) and Valine 4 (on the right). Note the atom numbers used in this paper.

the geometric structure of Valine 4 corresponds to the structure of the most stable valine conformer described in [14], while the conformer such as Valine 1 was not investigated in that paper. On the other hand, the study by Stepanian et al. [16] indicates the conformers selected for the investigation as most stable.

The calculated total energies and the ionization energies (IE) for the valine conformers are presented in Table 1. The measured differences in the ionization energies caused by the structural features of the molecule under study were obtained. It is well known that strong intramolecular H-bonds lead to higher IEs, and that is confirmed fairly well by our results, i.e. the IE of the Valine 1 conformer, where a hydrogen bond takes place, is larger than that of Valine 4. However, the total energy of the ionized Valine 1 conformer is lower than that of Valine 4 and indicates a lower thermal stability of this conformer.

The α -valine ionization was experimentally investigated in the photoionization studies of the parent ion yield curve showing a weak onset beginning at 8.9 eV and a large increase in the intensity beginning at 10.5 eV [17]. This paper also presents similar data by Klasinc [18], who gives the vertical IE(vert) = 9.68 eV and adiabatic IE(ad) = 8.71 eV ionization energy values. The last value is quoted in the NIST database [19].

Unfortunately, we failed to measure the IE of the initial valine molecule in our experiment due

to a vanishingly small intensity of the parent ion peak in the mass spectrum, but the calculated IE value for Valine 1 coincides well with the above experimental results.

Figure 2 shows the mass spectrum of the valine molecule measured by us at the 70 eV ionizing energy. The mass spectrum illustrates a general pattern of the positive fragment ions yield. There are no significant differences between the spectrum measured by us and those quoted in the NIST database for D- and DL-valine [19]. However, we obtained more pronounced ion production pattern at 27–30 a.m.u. Moreover, as mentioned above, there is no peak corresponding to the parent molecular ion yield, and this is related to a low stability of the ion produced during the ionization. This is typical for mass spectra of the aliphatic amino acids.

We have also measured the threshold energy dependences of the main fragment ion yields due to the electron impact on the valine molecule. The appearance energies (AE) for the main fragments produced due to electron impact on the valine molecule are the following: 12.4 eV for $C_3H_5N^+ + C_4H_7^+$; 12.0 eV for $C_4H_9^+ + C_3H_7N^+$; 9.5 eV for $C_4H_{10}N^+$; 10.1 eV for $C_2H_4NO_2^+$. The measured values are lower than those calculated theoretically. The experimental appearance energies were determined by means of the fitting technique suggested by T. Maerk's group (see details in, e.g. Ref. [20]) and used in most of our previous

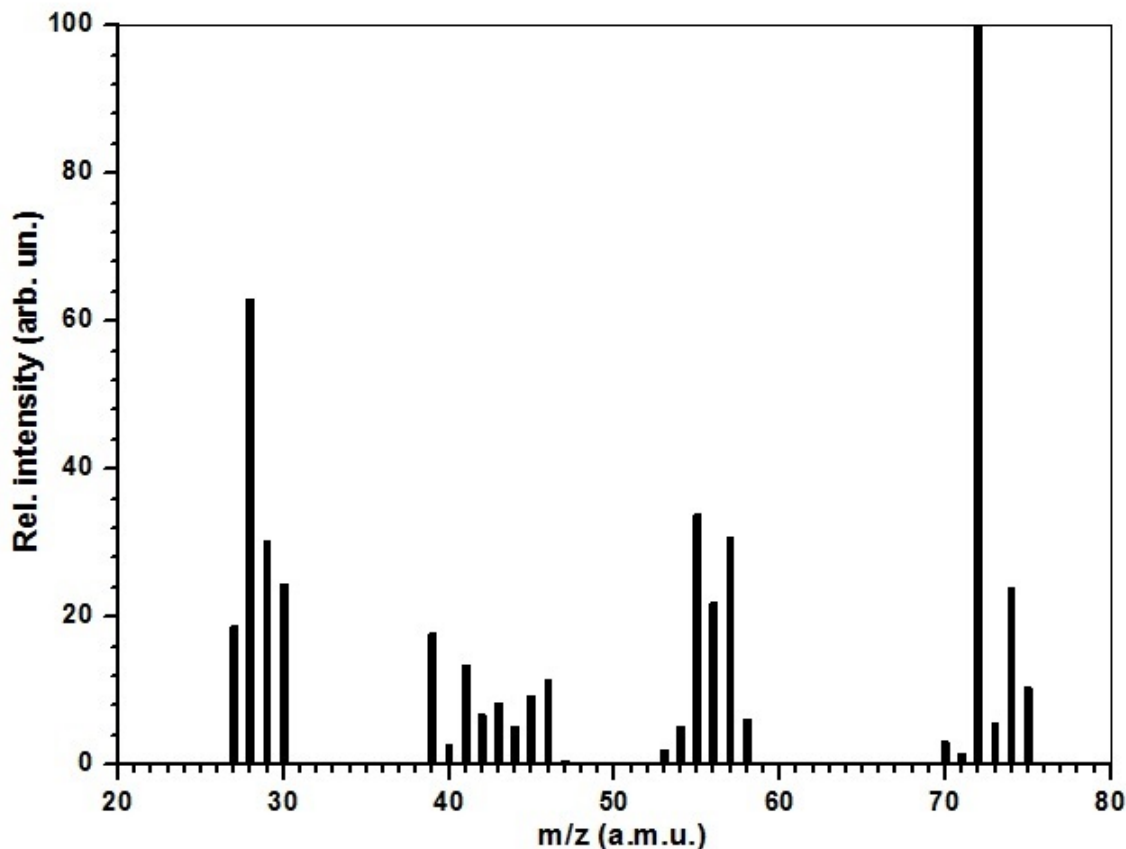


Fig. 2. Valine molecule mass spectrum.

studies. This technique is based on the least-squares method approximation using the Marquardt–Levenberg algorithm.

Obviously, the dissociation channel of the $C_5H_{11}NO_2$ molecule under the electron impact, common with most of α -amino acids, is due to the $C-C_\alpha$ bond break resulting in the formation of the $m/z = 72$ a.m.u. fragment, i.e. the most probable valine molecule dissociation process is due to the carboxyl group detachment.

The second (by its intensity) dissociation ionization channel relates to the production of the ions with the $m/z = 28$ a.m.u. mass. Several isobaric ions may correspond to this mass (i.e. CO, CNH_2 , C_2H_4), and their atomic composition determination requires an ultra high-resolution mass spectrometric technique. Besides the two main groups of the fragment ions in the vicinity of $m/z = 28$ and 72 a.m.u., the ions with the mass of $m/z = 39$ –46 a.m.u. and $m/z = 55$ –57 a.m.u. have noticeable intensities.

Let us recall that, in general, the incident free electron ionizes the target molecule to form a transitory ion. The parent precursor ion, having the in-

ternal energies below the dissociation energy, remains stable, whereas fragmentation may occur [10]. The ionization tends to cause the weakening of the bonding within the ion as compared to the neutral precursor. A weaker bonding means longer bond lengths in the average, and this goes with a higher tendency towards the bond dissociation. To estimate the changes in the valine molecule as a result of ionization, we calculated both the bond lengths and bond orders of the neutral and ionized valine conformers at their equilibrium point. Having taken into consideration the above facts and implemented the Mullikan population analysis data [21], the weakest bonds in the conformers of the molecule were determined. The calculated bond lengths and bond orders of both the neutral and ionized conformers of the valine molecule are listed in Tables 2 and 3.

According to the obtained results for the neutral and ionized conformers, the skeleton bonds C1–C3 and C1–C2 become weaker, while the C1–N7, C2–C10 and both C–O bonds become stronger due to the ionization. It should be noted that the mutual

Table 2. Bond lengths and bond orders of Valine 1 investigated before and after ionization.

Bond	Neutral		Ionized	
	Bond length, Å	Bond order	Bond length, Å	Bond order
C1–C2	1.551	0.966	1.544	0.931
C1–C3	1.539	0.880	1.721	0.645
C1–N7	1.473	0.805	1.378	1.118
C1–H19	1.094	0.916	1.086	0.890
C2–C10	1.532	0.985	1.530	0.994
C2–C11	1.535	0.970	1.539	1.015
C2–H12	1.095	0.923	1.099	0.871
C3–O4	1.342	1.043	1.309	1.055
C3–O5	1.201	1.960	1.180	1.983
O4–H6	0.982	0.753	0.969	0.768
N7–H8	1.010	0.876	1.011	0.820
N7–H9	1.012	0.869	1.011	0.826
C10–H13	1.091	0.944	1.089	0.925
C10–H14	1.087	0.944	1.090	0.925
C10–H15	1.092	0.941	1.091	0.918
C11–H16	1.090	0.954	1.089	0.926
C11–H17	1.092	0.937	1.091	0.922
C11–H18	1.091	0.951	1.089	0.934

locations of atoms in the conformational valine isomers strongly affect the bond length of the skeleton and the variation order. It may change noticeably the priority of the dissociation direction. For instance, in the case of the C1–C2 and C1–C3 bonds, which are weakened due to the ionization, the weakest bond for Valine 1 is C1–C3, while that for Valine 4 is C1–C2. Additionally, in both cases under study, the C–N bond becomes stronger resulting in the production of the fragments with the 27–30 a.m.u. masses occurring due to the simultaneous C1–C2 and C1–C3 bond dissociation and hydrogen atom migration. The variation of bond lengths and orders of the ionized conformers indicates a high probability of the C1–C3 bond dissociation of the molecular valine ion. Hence, it is not surprising that the most abundant ion in our experimental spectra is $C_4H_{10}N^+$ having the $m/z = 72$ a.m.u. mass. This fragment could be formed due to the C–C $_{\alpha}$ (C1–C3) bond cleavage (see Table 4).

The appearance energy for the fragment indicates that the dominant fragmentation pathway of the ionized valine molecule is associated with the loss of the negatively charged COOH that resulted in the 72 a.m.u. cation production. The min-

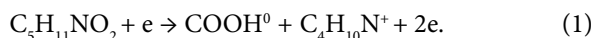
Table 3. Bond lengths and bond orders of Valine 4 investigated before and after ionization.

Bond	Neutral		Ionized	
	Bond length, Å	Bond order	Bond length, Å	Bond order
C1–C2	1.564	0.910	1.790	0.629
C1–C3	1.516	0.880	1.526	0.868
C1–N7	1.455	0.950	1.362	1.133
C1–H19	1.093	0.918	1.087	0.880
C2–C10	1.530	0.941	1.506	0.980
C2–C11	1.531	0.978	1.507	1.017
C2–H12	1.093	0.931	1.095	0.905
C3–O4	1.204	1.950	1.199	1.919
C3–O5	1.353	1.027	1.327	1.081
O4–H6	0.969	0.807	0.972	0.777
N7–H8	1.012	0.848	1.019	0.798
N7–H9	1.010	0.883	1.011	0.823
C10–H13	1.091	0.954	1.095	0.905
C10–H14	1.091	0.943	1.088	0.923
C10–H15	1.090	0.952	1.089	0.924
C11–H16	1.091	0.957	1.090	0.919
C11–H17	1.091	0.950	1.089	0.924
C11–H18	1.093	0.936	1.094	0.910

Table 4. Appearance energies of differently-charged COOH and C₄H₁₀N fragments.

COOH, $m/z = 45$ a.m.u.	C ₄ H ₁₀ N, $m/z = 72$ a.m.u.	Valine 1	Valine 4
-1	1	7.94	7.80
0	1	8.78	8.84
1	-1	12.31	12.34
1	0	11.53	11.53
1	1	16.95	16.94
0	-1	4.15	4.24

imal appearance energy of 7.94 or 7.80 eV for this fragment is lower than IE calculated for the case of the ion pair formation. It is interesting to compare the results of the calculations for this case made by us with the experimental results [15], where the third resonant peak for COOH⁻ corresponds to 7.9 eV at the dissociative electron attachment. However, above the ionization threshold, the neutral COOH fragment formation is more probable (as in the case of the majority of amino acids) via the following pathway:



It is interesting to note that the threshold for the [M-COOH]⁻ formation calculated in [22] is close to 4.1 eV at the G2MP2 level, which agrees well with the onset observed in both [15] and in our calculations.

The appearance energies for the $m/z = 45$ and 72 a.m.u. fragments indicate that the complementary COOH⁺ cations could provide only small mass spectrum intensities. The strong preference for the $m/z = 72$ a.m.u. fragment is ascribed to the ionization followed by the ejection of one electron from the unbound pair of electrons of the nitrogen atom; this process is the same as the one proposed for the ionization of amine molecules [23].

The experimentally measured AE of the C₄H₁₀N fragment is 9.5 ± 0.1 eV and is close to the calculated value for pathway (1).

Referring to the results presented in Tables 2 and 3, the cleavage of the O-H bond is the most probable fragmentation process combined with other fragmentation processes. It could lead to the formation of the differently charged COO and C₄H₁₀N fragments and the H atom. The results obtained prove the fact of formation of the C₄H₁₁N fragment, i.e. H may join the C₄H₁₀N molecule. However, in our

mass spectrum, as it is listed in the NIST database, the relative intensity of this ion peak is about 5% what corresponds exactly to the first isotopic peak for the C₄H₁₀N fragment. Hence, the $m/z = 73$ a.m.u. fragment peak in the mass spectrum at 70 eV could be assigned to the positively charged ¹³CC₃H₁₁N⁺ ion.

An unambiguous argument to prove this conclusion is the paper of Hu and Bernstein [24], where the isolated neutral amino acid molecules were ionized by single photons. In this work, the neutral ground state amino acid molecules were exposed to the IR radiation prior to the ionization, and the individual isomers were determined by observing the intensities for different fragments. Thus, in the time-of-flight mass spectra of valine ionized by the 10.5 eV energy photons with and without IR laser radiation (~ 3000 cm⁻¹) [24], the most prominent peaks correspond to the ions with the $m/z = 30, 72, 73$ and 84 a.m.u. masses. The authors concluded that, under conditions of their experiment, the amino acid molecule undergoes fragmentation due to the rearrangement reaction following the ionization stage. Such a rearrangement reaction in its simplest form could be a proton transfer and this reaction strongly depends on the internal hydrogen bonding, i.e. on the molecule conformation. Our relevant data on the appearance energy calculations are listed in Table 5.

Table 5. Appearance energies for differently charged COO and (C₄H₁₀N+H) fragments.

(C ₄ H ₁₀ N+H), $m/z = 73$	COO, $m/z = 44$	Valine 1	Valine 4
1	-1	8.78	9.99
1	0	7.88	9.09
1	1	21.64	22.85
-1	1	15.74	16.85
0	1	13.31	13.33

Low appearance energy values indicate a large possibility of the $C_4H_{11}N^+$ production in the process of the ion pair formation in the case of the neutral CO_2 fragment yield. So, we can conclude that the $C_4H_{11}N^+$ ion formation is energetically not probable at low energies due to the rearrangement processes.

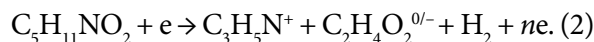
The cleavage of another weak C1–C2 bond in the valine molecule results in the formation of two complementary fragments, i.e. $C_2H_4NO_2$ with the $m/z = 74$ a.m.u. and C_3H_7 with $m/z = 43$ a.m.u. masses. The peak intensity of the first fragment obtained by different authors is nearly five times higher than that of the second one. In our spectrum, this ratio is about 4, so such an ion intensity distribution after the bond cleavage shows the preferable charge localization on the N-containing fragment. The results of our calculations of the appearance energies for the C_3H_7 and $C_2H_4NO_2$ fragments are listed in Table 6, while the AE value measured by us for the $C_2H_4NO_2$ fragment is 10.1 ± 0.1 eV. The analysis of the appearance energies proves the fact that the intensities of the peaks (or the abundance of their complementary fragments) is the isomer-conformation dependent. The difference between the appearance energies for the two conformers in a particular process is about 0.5 eV. This difference can be due to a feasible intramolecular hydrogen bonding between O5 and H14 in the case of Valine 1. When speaking about the appearance energy of the complementary fragments, the formation of the $C_2H_4NO_2$ fragment is energetically more preferable regardless of its charge.

Table 6. Appearance energies for the C_3H_7 and $C_2H_4NO_2$ fragments.

C_3H_7 , $m/z = 43$	$C_2H_4NO_2$, $m/z = 74$	Valine 1	Valine 4
1	-1	9.19	9.13
1	0	10.20	9.76
1	1	17.38	16.82
-1	1	10.68	10.21
0	1	10.03	9.47

Another intense peak in the valine mass spectrum corresponds to the $m/z = 55$ a.m.u. ion. There may be three isobaric ions with this mass: C_3H_5N , C_3H_3O and C_4H_7 . The process of C_3H_3O formation requires five skeleton bonds to be broken but this seems to be impossible. More probable is the for-

mation of the $C_3H_5N^+$ and the $C_4H_7^+$ ions. For $C_3H_5N^+$, three possible structures with the minimal total energy were calculated (see Table 7). All these ions are produced during the following process:

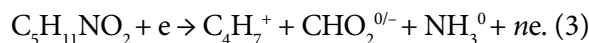


Here $n = 1, 2$ and '0/-' indicates that the fragment is neutral (0) or negatively charged (-).

Table 7. Total energies for the three structures of $C_3H_5N^+$.

Structure	Energy, a.u.
NCHCHCH ₃ ⁺	-171.721
NH ₂ CCCH ₃ ⁺	-171.786
NHCCHCH ₃ ⁺	-171.797

The last two structures have comparable total energies and our calculation of their appearance energies shows close values as well. The difference in the energies for similar conformers does not exceed 0.3 eV (see Table 8). The $C_4H_7^+$ fragment could be produced when one of the hydrogen atoms joins the amino group as follows:



Here $n = 1, 2$ and '0/-' indicates that the fragment is neutral (0) or negatively charged (-).

Table 8. Appearance energies for the two structures of $C_3H_5N^+$.

C_3H_5N , $m/z = 55$	$CHO_2 + CH_3 + H_2$	Valine 1	Valine 4
$H_2NCCCCH_3^+$	0	10.10	9.92
$HNCCHCH_3^+$	0	10.37	9.63

The analysis of the calculated appearance energy values (see Table 9) shows that the formation of the positively charged $m/z = 55$ a.m.u. fragment together with the negatively charged ($CHO_2 + NH_3$) compound is less energy-consuming. It should be noted that NH_3 is formed and both conformers have almost equal appearance energy values in every charge distribution case, so the C_4H_7 fragment formation does not depend on the conformation of the valine molecule. The analysis of the Mulliken charge indicates the negative charge location on CHO_2 . Moreover, the comparison of the binding

energy per atom of variously charged CHO_2 and NH_3 compounds indicates that the thermal stability of the neutral NH_3 (closed-shell system) is higher than that of the ionized one, but is smaller than that of the negatively charged COOH fragment (closed-shell system as well). The above data allowed us to predict the formation of the CHO_2^- fragment and the neutral NH_3 fragment when C_4H_7^+ is produced.

Table 9. Appearance energies for the positively charged C_4H_7 fragment.

C_4H_7 , $m/z = 55$ a.m.u.	$(\text{CHO}_2 + \text{H} + \text{NH}_3)$	Valine 1	Valine 4
1	-1	8.54	8.54
1	0	11.87	11.88
1	1	17.77	17.78

The value of the $m/z = 55$ a.m.u. ion appearance energy measured by us is 12.4 ± 0.1 eV. It is close to the calculated result in the case of the neutral $\text{CHO}_2 + \text{NH}_3$ fragment formation and it almost coincides with the experimental results and the G3MP2 calculations provided in [25].

The peak at $m/z = 56$ a.m.u. has also a noticeable intensity. The fragment could be formed similarly as the $m/z = 55$ a.m.u. one with no H12 loss. Referring to the results presented in Table 10, in the case of Valine 1 both fragmentation processes are possible:

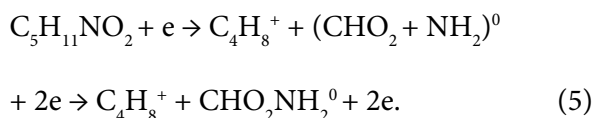
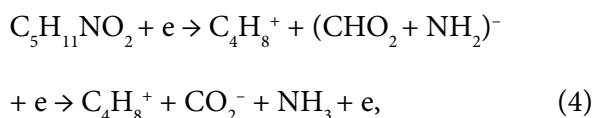


Table 10. Appearance energies for the positively charged C_4H_8 fragment.

C_4H_8 , $m/z = 56$ a.m.u.	$(\text{CHO}_2 + \text{NH}_2)$	Valine 1	Valine 4
1	-1	9.20	10.80
1	0	9.08	8.83
1	1	19.23	19.08

From the chemical point of view, the second pathway with a zero charge is preferable. In Ta-

ble 10, the appearance energies for the above products are presented; while in the case of Valine 4 the fragmentation according to scheme (5) is more favourable. It could occur due to the structural differences of the conformers. Only in the case of Valine 1 the placement of the product of fragmentation is favourable due to the H atom removal from the COOH group to form ammonia. Hence, the structural difference effect on the fragmentation process is evident.

The peak corresponding to the $m/z = 57$ a.m.u. fragment has its intensity comparable to that of the $m/z = 55$ a.m.u. one. Probably this peak indicates the presence of the C_4H_9 , C_2HO_2 , $\text{C}_2\text{H}_3\text{NO}$ or $\text{C}_3\text{H}_7\text{N}$ positively charged ions. The formation of C_2HO_2^+ was assumed in [26], where other products of the process were the neutral NH_3 and $(\text{CH}_3)_2\text{CH}^*$ radicals, so the authors supposed the dissociation of the C1–N7 and C1–C2 skeleton bonds. This ion can exist in the case of a rearrangement of the $\text{HO-C}^*=\text{C}=\text{O}$ structure, which seems to be a very unfeasible event under the conditions of our experiment.

Another composition of the ion with $m/z = 57$ a.m.u. is $\text{C}_2\text{H}_3\text{NO}$, formed after the detachment of $(\text{CH}_3)_2\text{CH}$ and the water molecule, made of H from the amino group and OH from the acetic one. This mechanism of the $\text{C}_2\text{H}_3\text{NO}^+$ ion formation was proposed by Junk and Svec [23] and Jochims et al. [17], and confirmed by Papp et al. [15, 25] when two possible cases of the residual fragment structure were studied.

We would like to emphasize that the formation of NHCHCOH with the minimal number of possible reactions could occur due to the cleavage of the C1–C2, C–OH and N–H bonds after the H8 atom migration to O5. Meanwhile, to form the C_4H_9 positively charged ion, the C1–C3 and C1–N4 bonds should be cleaved and the H atom, due to the deprotonation of COOH , may join the C_4H_8 fragment. The C1–C2 and O–H bonds become weaker due to the tendency of the ionization process of valine to be destructed; the C1–N4 bond is weaker than the C3=O5 one (see Tables 1 and 2). On the other hand, the residual isobaric ion with the $m/z = 57$ a.m.u. mass, i.e. $\text{C}_3\text{H}_7\text{N}^+$, is formed due to the cleavage of the C1–C3 and C2–C10 bonds only. This allows us to predict that formation of NHCHCOH could require a larger energy amount than that of C_4H_9 or $\text{C}_3\text{H}_7\text{N}$.

The thermal stability of the C_3H_7N positively charged fragments (with the binding energy per atom of 3.79 eV) and C_4H_9 , (with the binding energy per atom of 3.61 eV) is not quite different. The appearance energy of these two fragments is also not significantly different, although it depends on the isomer conformation (see Tables 11, 12). It should be noted that the process of the C_3H_7N ion formation with the neutral counterpart production (see pathway (6)) is as follows:

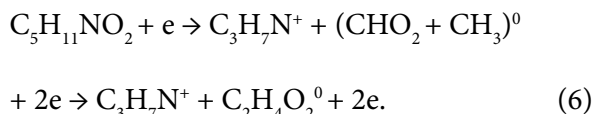


Table 11. Appearance energies for the positively charged C_4H_9 fragment.

C_4H_9 , $m/z = 57$ a.m.u.	$CO_2 + NH_2$	Valine 1	Valine 4
1	-1	7.40	9.20
1	0	10.17	11.96
1	1	20.10	21.90

Table 12. Appearance energies for the positively charged C_3H_7N fragment.

C_3H_7N , $m/z = 57$ a.m.u.	$CHO_2 + CH_3$	Valine 1	Valine 4
1	-1	8.06	9.20
1	0	8.04	11.96
1	1	18.97	18.27

The data of Tables 11 and 12 unambiguously show the effect of conformational differences on the fragmentation process. The *trans*- or the *cis*- position of the hydroxyl group hydrogen with respect to the amino group and intramolecular hydrogen bonding can lead to the difference of about 1 eV in the appearance energy for the $m/z = 57$ a.m.u. ion.

We also calculated the appearance energy for two possible structures of the $C_2H_3NO^+$ ion reported in [17, 15, 24, 25] as the main composition for the $m/z = 57$ a.m.u. ion. The total energies of both structures are presented in Table 13. The minimal appearance energy for the first structure is 12.41 eV, while those for the second one are 9.54 eV for Valine 1 and 10.02 eV for Valine 4 (all results are for the neutral counterparts). So, compared to the measured by us threshold for the $m/z = 57$ a.m.u. ion of 12.0 eV, we assume that

at this energy all the C_4H_9 , C_2H_3NO , and C_3H_7N ions can exist.

Table 13. Total energies for the two structures of the $C_2H_3NO^+$ ion.

Structure	Energy, a.u.
NHCHC(OH) ⁺	-207.641
NH ₂ CHCO ⁺	-207.7415

In the mass spectrum region of $m/z = 25$ – 30 a.m.u., there are three intensive peaks corresponding to $m/z = 28$, 29 and 30 a.m.u. The most intensive peak of this group corresponds to the $m/z = 28$ a.m.u. fragment. Three isobaric ions, CH_2N^+ , $C_2H_4^+$ and CO^+ , can match this mass. For some amino acid molecules we proved that the HCNH fragment requires less energy to appear than the CO^+ one [26]. Papp et al. [15] demonstrated that the calculated appearance energy for CO^+ (15.01 eV) is about 3 eV higher than that for CH_2N^+ (11.87 eV). Our calculations for the CO^+ appearance energy are practically identical with those presented in [15], i.e. 15.31 eV for Valine 1 and 15.01 eV for Valine 4. It is necessary to mention that the formation of $m/z = 28$ with the C_2H_4 chemical composition via different pathways was investigated as well. However, the stability of the CH_2N^+ fragment is larger than that of the $C_2H_4^+$ one, indicated by the binding energy per atom. The comparison of the appearance energies for these two fragments proves the formation of CH_3N^+ as energetically more favourable. It allows us to conclude that the positively charged $m/z = 28$ a.m.u. fragment is HCNH. The assignment of the intense peak at $m/z = 28$ a.m.u. to HCNH was also confirmed by observing the $m/z = 29$ a.m.u. mass peak in the α -valine-d3 ($ND_2(CH_3)_2(CH)_2COOD$) by Jochims et al. [17]. We unambiguously calculated the minimal energy required to produce the $m/z = 28$ a.m.u. ion with the CH_2N chemical composition. Referring to the results presented in Table 14, the minimal energy consumption for this fragment appearance corresponds to the ion pair formation. However, the appearance energy for the $m/z = 28$ a.m.u. fragment obtained experimentally by Papp et al. [15] is 13.1 eV. The calculated value of 12.45 eV fits this measurement better. Hence, the $m = 28$ a.m.u. fragment could be formed according to the scheme:

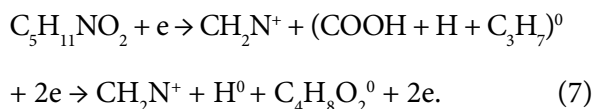
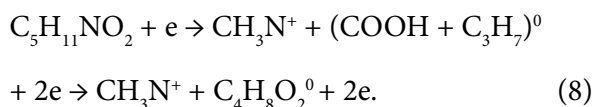


Table 14. Appearance energies for the HCNH fragment.

CH_2N , $m/z = 28$ a.m.u.	$\text{COOH} + \text{H} + \text{C}_3\text{H}_7$	Valine 1	Valine 4
1	-1	9.10	9.87
1	0	12.45	12.22
1	1	17.61	18.43

The fragment with $m/z = 29$ a.m.u. could be produced in a simpler way, i.e. due to the cleavage of the C1–C3 and C1–C2 bonds without the NH_2 deprotonation (see Table 15):

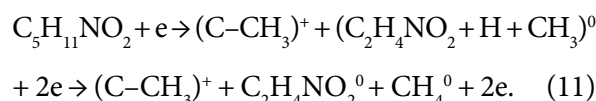
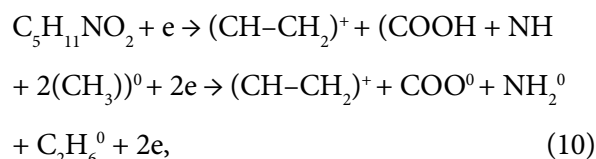
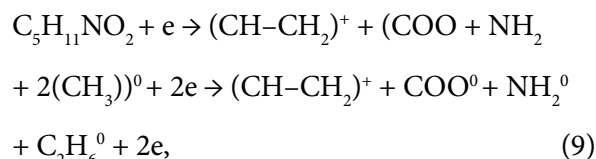
Table 15. Appearance energies for the HCNH_2 fragment.

CH_3N , $m/z = 29$ a.m.u.	$\text{COOH} + \text{C}_3\text{H}_7$	Valine 1	Valine 4
1	-1	11.89	11.68
1	0	10.58	10.35
1	1	20.44	20.33

In the mass spectrum, the peak of the $m/z = 28$ a.m.u. ion is larger than that of $m/z = 29$ a.m.u., despite the fact that the latter ion needs less bonds to be broken and in the case of neutral counterpart production the energy consumption is less as well. However, the binding energy per atom for

CH_2N^+ is equal to 2.77 eV and is larger than that of 2.48 eV for CH_3N^+ . Hence, the thermal stability of the CH_2N cation is larger than that of CH_3N . Moreover, the HOMO-LUMO gap analysis of these two fragments indicates that the CH_2N ion is chemically more stable than the CH_3N^+ one. It allows us to predict that some CH_2N positively charged fragments could be produced by the CH_3N^+ deprotonation and the secondary fragmentation process as well.

The fragment with $m/z = 27$ a.m.u. can have two chemical compositions. They could be CHN or C_2H_3 and the binding energy per atom for them is 1.62 and 2.54 eV, respectively. Hence, the thermal stability of C_2H_3 is larger than that of CHN . The calculated fragment appearance energy is smaller than that for CHN (Tables 16, 17), thus leading to the conclusion that at the threshold electron energy the $m/z = 27$ a.m.u. fragment is C_2H_3 . This ion can have two structures, i.e. CH-CH_2^+ with the total energy of -77.616 a.u. and C-CH_3^+ with that of -77.540 a.u. We have calculated three possible ways of the C_2H_3 fragment formation: with different final products and for the cases when it consists of the C1–C2 and C2–C10 (11) carbon atoms (see pathways 9–11):

Table 16. Appearance energies for the C_2H_3 fragment.

$m/z = 27$ a.m.u.	Counterparts	Valine 1	Valine 4
CH-CH_2	$\text{COO} + \text{NH}_2 + 2(\text{CH}_3)$	13.12	13.13
CH-CH_2	$\text{COOH} + \text{NH} + 2(\text{CH}_3)$	13.12	13.47
C-CH_3	$\text{C}_2\text{H}_4\text{NO}_2 + \text{H} + \text{CH}_3$	14.52	14.58

Table 17. Appearance energies for the HCN fragment.

CHN , $m/z = 27$ a.m.u.	$(\text{COOH} + \text{H} + \text{CH}(\text{CH}_3))$	Valine 1	Valine 4
1	-1	15.93	19.78
1	0	14.37	18.58
1	1	24.26	28.57

The results of our calculations for the neutral counterparts are presented in Table 16. One can see that only in the case of COOH + NH as the other products are also formed, a marked difference in the appearance energy for the valine molecule conformers is present. So, the H-atom transition from the COOH-group to C2 is practically not dependent on the conformer structure, but in the case of H originating from NH₂ the difference in the energies is approximately equal to the hydrogen binding energy. This can give evidence of the presence of the H8•••O4 hydrogen bond in Valine 4.

The HCN fragment formation is more energy-consuming (see Table 17) as compared to that for C₂H₃, so the C₂H₃ ion with the $m/z = 27$ a.m.u. is more likely to appear at the threshold energy. It should be noted that the $m/z = 27$ a.m.u. ion was considered as C₂H₃ by Denifl et al. [22] and Jochims et al. [177] as well.

5. Conclusions

The analysis of the valine molecule mass spectrum together with the theoretical calculations was performed. The results obtained allowed us to determine the main dissociation mechanisms of the conformers of this molecule under a low-energy electron impact. The appearance energies for the most pronounced ion peaks in the valine molecule mass spectrum were measured experimentally and estimated theoretically. Despite the fact that there are no significant differences between our measured spectrum and those quoted in the NIST database, we obtained a more pronounced ion product pattern at 27–30 a.m.u. Our experimental mass spectrum also indicates the low stability of the parent molecular ion.

The dominant fragmentation pathway of the ionized valine molecule is related to the C–C_α bond cleavage with a loss of a neutral COOH fragment, as in the case with most of α-amino acids and the C₄H₁₀N⁺ ion production. The calculated appearance energies for this pathway showed almost a full absence of the structural influence on this process.

As for some other fragments, the difference between their appearance energies from the two conformers of valine indicates a significant influence of a feasible intermolecular hydrogen bonding. The *trans*- or the *cis*- position of the hydroxyl

group hydrogen with respect to the amino group and intramolecular hydrogen bonding can lead to the difference in the appearance energy of about 1 eV or more (for $m/z = 57$ a.m.u. ion and, especially, for CHN⁺). The formation of ammonia is also probable in the case of the conformer where a hydrogen bond is present. However, the formation of some fragments (for example, C₄H₇) is independent of the valine molecule conformation. The results obtained lead to the prediction that the influence of the hydrogen bond, i.e. the structural differences, could be significant in the case of the formation of some fragments.

It is interesting that the H atom transition from the COOH group is independent of the conformer structure, but in the case of H origination from the NH₂ group, the difference in the appearance energies has the order of magnitude approximately equal to the hydrogen bond energy.

Additionally, different structural and chemical compositions of the isobaric fragments of valine formed under electron impact were determined and analysed.

Acknowledgements

The authors would like to greatly appreciate the fruitful cooperation with Prof. M. Cegla (Jagellonian University, Krakow, Poland). This work was carried out within the framework of the UNAS (the National Academy of Sciences of Ukraine) as Young Scientist Grant for the support of both experimental and theoretical research, as well as within the COST MP0802 and COST XLiC programmes.

References

- [1] B. Boudaïffa, P. Cloutier, D. Hunting, M.A. Huels, and L. Sanche, Resonant formation of DNA strand breaks by low-energy (3 to 20 eV) electrons, *Science* **287**, 1658 (2000).
- [2] J.F. Ward, in: *Advances in Radiation Biology*, Vol. 5, eds. J.T. Lett and H. Adler (Academic Press, New York, 1977) pp. 181–239.
- [3] A. Sak, M. Stuschke, R. Wurm, and V. Budach, Protection of DNA from radiation-induced double-strand breaks: influence of replication and nuclear proteins, *Int. J. Radiat. Biol.* **76**, 749 (2000).

- [4] A. Valota, F. Ballarini, W. Friedland, P. Jacob, A. Ottolenghi, and H.G. Paretzke, Modelling study on the protective role of OH radical scavengers and DNA higher-order structures in induction of single- and double-strand break by gamma-radiation, *Int. J. Radiat. Biol.* **79**, 643 (2003).
- [5] S. Denifl, I. Mähr, F. Ferreira da Silva, F. Zappab, T.D. Märk, and P. Scheier, Electron impact ionization studies with the amino acid valine in the gas phase and (hydrated) in helium droplets, *Eur. Phys. J. D* **51**, 73 (2009).
- [6] C. Michaux, J. Wouters, D. Jacquemin, and E.A. Perpète, A theoretical investigation of the hydrated glycine cation energetics and structures, *Chem. Phys. Lett.* **445**, 57 (2007).
- [7] V.S. Vukstich, A.I. Imre, L.G. Romanova, and A.V. Snegursky, Fragmentation of the glycine molecule by low-energy electrons, *J. Phys. B* **43**, 185208-1 (2010).
- [8] V.S. Vukstich, A.I. Imre, and A.V. Snegursky, Modernization of the MII201 mass spectrometer for studying the electron–molecule interaction processes at low electron energies, *Instr. Exper. Tech.* **54**, 66 (2011).
- [9] V.S. Vukstich, L.G. Romanova, I.G. Megela, and A.V. Snegursky, Mass-spectrometric study of the electron-impact-induced fragmentation of the tryptophan molecule, *Tech. Phys. Lett.* **40**, 263 (2014).
- [10] A. Kraj, D.M. Desiderio, and N.M. Nibbering, in: *Mass Spectrometry: Instrumentation, Interpretation, and Applications*, eds. R. Ekman, J. Silberring, A. Westman-Brinkmalm (John Wiley & Sons, 2009) p. 388.
- [11] A.D. Becke, Density-functional thermochemistry. III. The role of exact exchange, *J. Chem. Phys.* **98**, 5648 (1993).
- [12] R.A. Kendall, T.H. Dunning Jr., and R.J. Harrison, Electron affinities of the first-row atoms revisited. Systematic basis sets and wave functions, *J. Chem. Phys.* **96**, 6796 (1992).
- [13] J.T. Bursey, M.M. Bursey, and D.G.I. Kingston, Intramolecular hydrogen transfer in mass spectra. I. Rearrangements in aliphatic hydrocarbons and aromatic compounds, *Chem. Rev.* **73**, 191 (1973).
- [14] S. Dokmaisorijan, V.S. Lee, and P. Nimmanpipug, The gas phase conformers and vibrational spectra of valine, leucine and isoleucine: An ab initio study, *J. Mol. Struct. Theochem* **953**, 28 (2010).
- [15] P. Papp, J. Urban, Š. Matejčík, M. Stano, and O. Ingólfsson, Dissociative electron attachment to gas phase valine: A combined experimental and theoretical study, *J. Chem. Phys.* **125**, 204301 (2006).
- [16] S.G. Stepanian, I.D. Reva, E.D. Radchenko, and L. Adamowicz, Combined matrix-isolation infrared and theoretical DFT and ab initio study of the nonionized valine conformers, *J. Phys. Chem. A* **103**, 4404 (1999).
- [17] H.-W. Jochims, M. Schwell, J.-L. Chotin, M. Clemino, F. Dulieu, H. Baumgärtel, and S. Leach, Photoion mass spectrometry of five amino acids in the 6–22 eV photon energy range, *Chem. Phys.* **298**, 279 (2004).
- [18] L. Klasinc, Application of photoelectron spectroscopy to biologically active molecules and their constituent parts: III. Amino acids, *J. Electron Spectrosc. Relat. Phenom.* **8**, 161 (1976).
- [19] *NIST Chemistry WebBook*, <https://webbook.nist.gov>
- [20] G. Hanel, B. Gstir, T. Fiegele, F. Hagelberg, K. Becker, P. Scheier, A.V. Snegursky, and T.D. Märk, Isotope effects in the electron impact ionization of H_2/D_2 , $\text{H}_2\text{O}/\text{D}_2\text{O}$ and $\text{C}_6\text{H}_6/\text{C}_6\text{D}_6$ near threshold, *J. Chem. Phys.* **116**, 2456 (2002).
- [21] R.S. Mulliken, Electronic population analysis on LCAO-MO molecular wave functions. I, *J. Chem. Phys.* **23**, 1833 (1955).
- [22] S. Denifl, H.D. Flosadóttir, A. Edtbauer, O. Ingólfsson, T.D. Märk, and P. Scheier, A detailed study on the decomposition pathways of the amino acid valine upon dissociative electron attachment, *Eur. Phys. J. D* **60**, 37 (2010).
- [23] G. Junk and H. Svec, The mass spectra of the α -amino acids, *J. Am. Chem. Soc.* **85**, 839 (1963).
- [24] Y. Hu and E.R. Bernstein, Vibrational and photoionization spectroscopy of biomolecules: Aliphatic amino acid structures, *J. Chem. Phys.* **128**, 164311 (2008).

- [25] P. Papp, P. Shchukin, J. Koříšek, and Š. Matejíček, *J. Chem. Phys.* **137**, 10510-1 (2012).
- [26] A.F. Lago, L.H. Coutinho, R.R.T. Marinho, A. Naves de Brito, and G.G.B. de Souza, Ionic dissociation of glycine, alanine, valine and proline as induced by VUV (21.21 eV) photons, *Chem. Phys.* **307**, 9 (2004).

JONIZUOJANČIOSIOS SPINDULIUOTĖS ĮTAKA AMINORŪGŠČIŲ MOLEKULĖMS: VALINO ATVEJIS

J. Tamulienė^a, L. Romanova^b, V. Vukstich^b, A. Papp^b, L. Baliulytė^a, A. Snegursky^b

^a *Vilniaus universiteto Teorinės fizikos ir astronomijos institutas, Vilnius, Lietuva*

^b *Ukrainos nacionalinės mokslų akademijos Elektronų fizikos institutas, Užgorodas, Ukraina*

Santrauka

Darbe pateikti nauji valino molekulės ($C_5H_{11}NO_2$) fragmentacijos dėl žemos energijos elektronų, atsirandančių esant jonizuojančiai spinduliuotei, poveikio tyrimai. Pateikiame eksperimentiškai išmatuotas valino fragmentų atsiradimo energijos vertes ir masės spektrą. Taikant tankio funkcionalo teorijos B3LYP/cc-pVTZ ar-

tinį, buvo patikslinta minėtame masės spektre matomų fragmentų cheminė sudėtis ir geometrinė struktūra bei įvertinta jų atsiradimo energija. Atlikus gautų teorinių ir eksperimentinių rezultatų analizę, nustatytos tikimiausios valino molekulių suskaidymo reakcijos, kurios taip pat pateiktos šiame darbe.